Influence of Swirl on the Discharge Coefficients of Sonic Nozzles

Seong-Yeon Yoo*, Kee-Young Yoon and Kyung-Am Park*****

(*Received October 25, 1996*)

Flow characteristics of a swirl generator are studied using an open circuit flow loop, and influence of upstream swirl on the discharge coefficients of sonic nozzles is investigated using a high pressure gas flow standard measurement system. The open circuit flow loop consists of swirl generator, testsection, sonic nozzle, suction fan and LDV system. The gas flow measurement system comprises two compressors, storage tank, temperature control loop, sonic nozzle testsection, weighing tank, gyroscopic scale and data acquisition system. Experiments are performed at various nozzle throat diameters, inlet pressures and angles of swirl generator. As the angle of swirl generator becomes larger, axial velocities decrease near the wall and rapidly increase in the pipe core, and swirl velocities increase to form swirl flow. Influence of upstream swirl on discharge coefficients becomes greater as the intensity of swirl increases and as the nozzle throat diameter is enlarged. Variation trend with Reynolds number, however, is very similar each other regardless of swirl intensity.

Key Words: Sonic Nozzle, Discharge Coefficients, Swirl, Gas Flow Measurement

Nomenclature

A : Cross sectional area of nozzle throat
C_* : Critical flow function of ideal gas
C_d : Discharge coefficient
m : Mass of air passed through sonic nozzle
m' : Indicated mass by gyroscopic scale
M : Molecular weight of air
P_0 : Stagnation pressure
R : Gas constant
Re : Reynolds number based on nozzle throat diameter
t : Air collection time
T_0 : Stagnation temperature
V_d : Volume of air displaced by weighing tank
V_L : Volume of pipeline between nozzle throat and stop value at inlet of weighing tank
$\rho_{atm,1}$: Density of air at atmospheric pressure before test run
$\rho_{atm,2}$: Density of air at atmospheric pressure after test run
ρ_1 : Density of air in the pipeline before test run
ρ_2 : Density of air in the pipeline after test run
y : Radial distance in the velocity measurement domain
z : Axial distance in the velocity measurement domain
r_0 : Inner radius of test-section

* Mechanical Design Engineering, Chungnam National University, Taejon, 305-764, Korea
** Taejon-Chungnam Regional Small and Medium Business Office, Taejon, 300-092, Korea
*** Fluid Flow Lab., Korea Research Institute of Standards and Science, Taejon, 305-606, Korea

1. Introduction

Consumption of natural gas is growing very rapidly during the past several decades. For the fair commercial trade and for the more efficient system operations, accurate measurement of the gas flow rate has become an activity of great importance. A critical sonic nozzle has many advantages in the measurement and control of the

gas flow. As long as sonic nozzle conditions exist in the nozzle throat, the mass flow rate is steady and can be expressed as a function of the upstream pressure and temperature. The advantage also includes operational simplicity and high potential accuracy. It is usually assumed that the gas flowing through a sonic nozzle is one dimensional and isentropic. However actual gas flow conditions are somewhat different from those of ideal gas, which is caused by frictional loss, boundary layer formation, heat transfer, real gas effects, and etc. Such deviations can be handled by applying discharge coefficients.

Arnberg (1962) reviewed critical flowmeters for gas flow measurements. Discussions were made on theoretical flow functions, parameters correlating discharge coefficients, and the importance of real gas properties. Brown and et. al. (1985) examined three critical venturi designs from the stand point of their sensitivity to initial boundary layer thickness, inlet flow nonuniformity, separation and transition point location. Smith and Matz (1962) suggested a theoretical method of determining discharge coefficients, and compared theoretically and experimentally determined coefficients. Johnson (1964) studied with computer simulation how to modify the conventional one dimensional equations for mass flow of air, nitrogen, oxygen, hydrogen, argon, helium, and steam through a nozzle for taking into account the real gas effects. Effects of flow straightener on discharge coefficients have been examined by Blake et. al. (1981). Kinghorn et. al. (1991) determined the optimum length of étoile-type straightener for removing the non-axial velocity component from swirling flows.

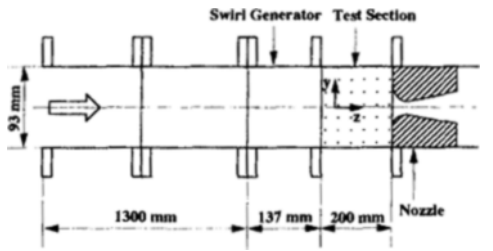

Fig. 1 A schematic diagram of an open circuit flow loop

The purpose of this research is to investigate upstream swirl which influences the discharge coefficients of sonic nozzle. Flow characteristics of a swirl generator are measured using an open circuit flow loop with LDV system, and influence of upstream swirl on the discharge coefficients of sonic nozzle is investigated using high pressure gas flow standard measurement system with gyroscopic scale. Experiments are performed with various nozzle throat diameters, inlet pressures and angles of swirl generator.

2. Experimental Apparatus and Procedures

2.1 Open circuit flow loop

An open circuit flow loop, shown in Fig. 1, comprises swirl generator, test-section, sonic nozzle, suction fan and LDV system. The sonic nozzle used in this experiment has a throat diameter of 16.980 mm. Swirl generator, shown in Fig. 2, is made of four movable plate vanes. The intensity of swirl is controlled by a vane angle, which is the angle between flow direction and vane plane. When the vane angle is 0° or 90°, the swirl generator is fully open or closed, respectively. Test-section is made of glass, and its length and diameter are 200 mm and 93 mm, respectively. A suction fan is connected to the flow loop using a flexible joint, and flow velocity is controlled by adjusting the input voltage of the suction fan.

The LDV system consists of power supply,

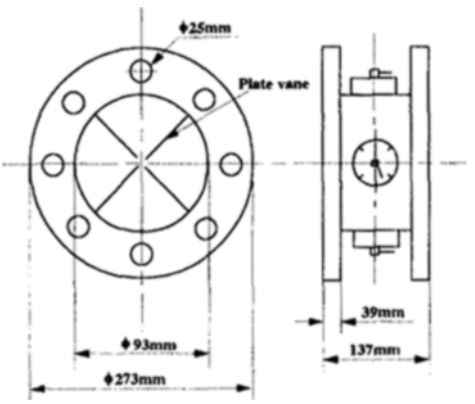

Fig. 2 A schematic diagram of swirl generator

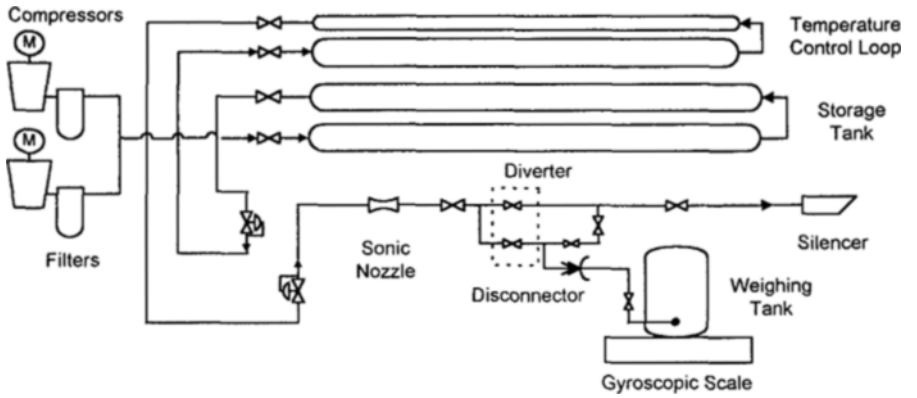

Fig. 3 A schematic diagram of high pressure gas flow standard measurement system

multicolor beam separator, multicolor receiver, signal processor, traverse table, seed generator and PC. This system uses 5W argon-ion laser and laser source is water-cooled. To obtain adequate data rates and good signal quality, Polystyrene Latex particles are fed into the flow 1437 mm upstream from the test-section. Spherical shape Polystyrene Latex particles have density of 1.05g/cc, refractive index of 0.59 and mean diameter of 0.993 m $\pm$0.021 μm.

2.2 High pressure gas flow standard measurement system

The high pressure gas flow standard measurement system, shown in Fig. 3, comprises two compressors, storage tank, temperature and pressure control loop, sonic nozzle testsection, weighing tank, gyroscopic scale and data acquisition system. Two compressors of a free air delivery 0.033 m^3/s and an outlet pressure of 7.1 MPa were used to fill the storage tank of 20 m^3 up to 6.5 MPa. The storage tank was made of two circular cylinders. The length and diameter of the cylinder are 30 m and 0.66 m, respectively. In order to establish stable temperature and pressure conditions in the test-section during the test run, the air from the storage tank is regulated to about 5 MPa and then stored in the temperature control loop until the air temperature is stabilized. The total length of the loop is about 45 m and its volume is 7 m^3.The air from the temperature control loop is regulated again to a working pressure and discharged into the test line. The air passed through

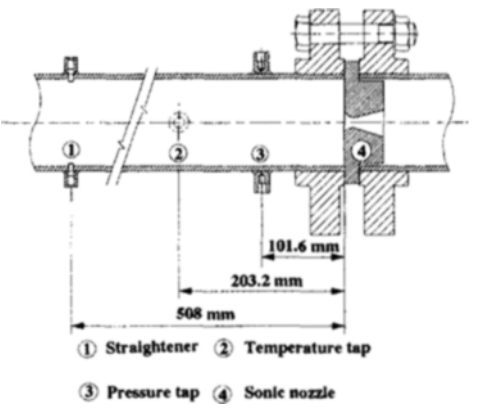

Fig. 4 A schematic diagram of sonic nozzle test-section

the sonic nozzle package can be directed either to the open air via a silencer or to the weighing tank placed on a gyroscopic scale. A sonic nozzle package is fabricated according to Draft International Standard ISO/DIS 9300 as shown in Fig. 4.

The weighing tank is connected and disconnected by a specially designed coupling to the pipeline before and after the collection of the test air, respectively. The weighing tank is a 2 m^3 cylindrical shape, and is capable of withstanding pressure up to 4.5 MPa and temperature in the range of -10 ℃ to 40 ℃. The weighing tank is balanced on a gyroscopic scale which can measure 100 kg of air with 5 g resolution. For accurate measurement of the mass of air passed through the critical sonic nozzle, compensation has to be made for unweighed air contained in the pipeline between the nozzle and the stop valve at

the weighing tank inlet. The volume of the unweighed air, amounts to 0.8 % of volume of the weighing tank, has been determined within ±1 % by volume measurement. The pressure and temperature of the air contained in the pipeline was recorded at the beginning and end of each diversion to determine the mass of the unweighed air.

2.3 Data acquisition system

The data acquisition hardware and software developed for the flow standard system provide a comprehensive and rapid mean in collecting flow-related data over a full range of operating conditions. The pressure upstream of the sonic nozzle is measured with a Ruska quartz pressure gage. The output of the quartz pressure gage is then sent to the data acquisition system. Pressure at the pipeline between the divert and the stop valve is measured with a Heise precision pressure gage. The pressure monitoring console consisted of 6 Bourdon gages monitors pressures at the outlet of compressors, the storage tank, the temperature control loop, and the testline. The atmospheric pressure is measured with a digital barometer.

Two high precision PRT sensors are used to measure the temperatures upstream of the sonic nozzle and in the pipe connected to the weighing tank. Another three PRT sensors are installed at the storage tank, the temperature control loop, and the testline. The collection time of the air in the weighing tank is measured with a counter triggered by a photo-interrupter in diverting system. All instruments including the gyroscopic scale indicator are connected to the data acquisition system. The software for data acquisition is developed to interface instruments and to perform necessary calculations.

3. Results and Discussion

3.1 Flow characteristics of swirl generator

An open circuit flow loop with swirl generator is used to investigate the flow characteristics of swirl. Experiments are performed at various angles of swirl generator. Figure 5 shows the distribution of axial and swirl velocities in front of the nozzle inlet at z=130 mm (50 mm upstream from the nozzle inlet). For the angle of 0° and 20°, velocity distributions are similar to the turbulent pipe flow, and main flow seems to be disturbed weakly by the swirl generator. As the angle of swirl generator increases, the axial velocity, however, decreases around $y/r_0 \approx \pm 0.5$, and increases remarkably in the core. As shown in Fig. 5(b), the swirl velocity increases from the centerline, reaches a maximum around $y/r_0 \approx \pm 0.3$, and decreases to the zero later on. The intensity of swirl becomes greater as the angle of swirl generator increases. Apparent swirling flow appears for the angle of swirl generator larger than 40°, and this flow influences the discharge coefficients of the sonic nozzle.

Figure 6 shows the variation of axial velocity

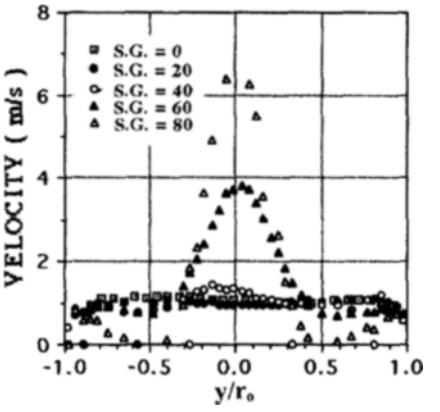

(a) Axial velocity

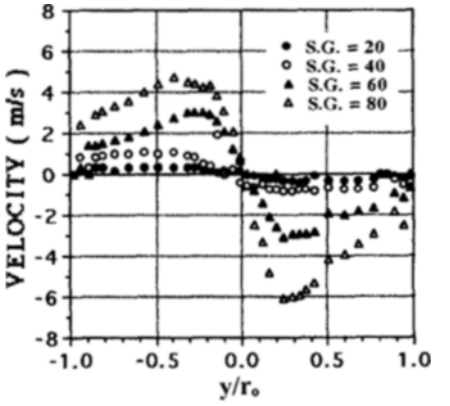

(b) Swirl velocity

Fig. 5 Velocity distributions of swirling flow for the various angles of swirl generator (z=130 mm)

along the centerline for the swirl generator angle of 0° and 60°. Without swirl (i.e.S.G.=0°), axial velocity increases slightly when the flow approaches to the nozzle. This acceleration is mainly due to the change of flow area. There must be a dead zone just upstream of the nozzle because nozzle throat diameter is much smaller than the pipe diameter as shown in Fig. 1. It is evident from the figure that the flow acceleration is much faster in the case of swirling flow (i.e.S. G.=60°). Axial and swirl velocity changes along the streamwise direction are presented in Fig. 7 at the different radial locations for the swirl generator angle of 60°. In the location where y/r_0 is 0. 484 and 0.742, axial and swirl velocities are almost uniform. But slight decrease in both velocities is seen in the latter part of the test-section in the case of y/r_0=0.742.Axial and swirl velocities increase in the core region, and the acceleration is faster as r/r_0 becomes smaller.

3.2 Accuracy of discharge coefficient measurement

The ideal mass flow rate of the sonic nozzle is determined by the following equation.

$$\dot{m}_{ideal}=\frac{C_* A P_0}{(RT_0)^{0.5}} \tag{1}$$

In the actual gas flow, however, one dimensional-isentropic condition is broken by frictional loss, boundary layer formation, heat transfer, and etc. Besides the equation of state of real gas is different from that of ideal gas, and the specific heat ratio of real gas is a function of temperature. The actual mass flow rate of sonic nozzle is given by

$$\dot{m}=C_d\dot{m}_{ideal}=C_d\frac{C_* A P_0}{(RT_0)^{0.5}} \tag{2}$$

The discharge coefficient C_d represents the deviation from ideal condition. In this research, the high pressure gas flow standard measurement system is used to investigate the characteristics of the discharge coefficients of sonic nozzles.

The mass flow rate in the system is measured by

$$\dot{m}=\frac{m}{t}$$

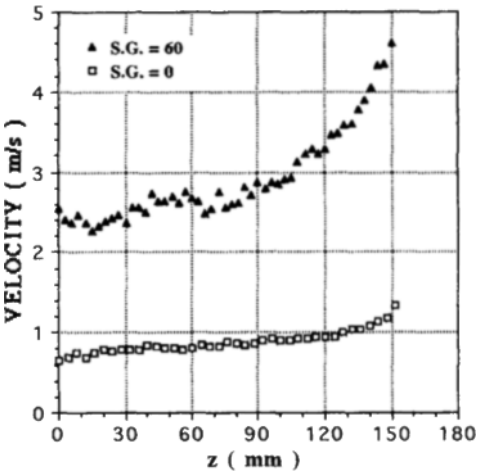

Fig. 6 Comparison of axial velocity variation along the centerline

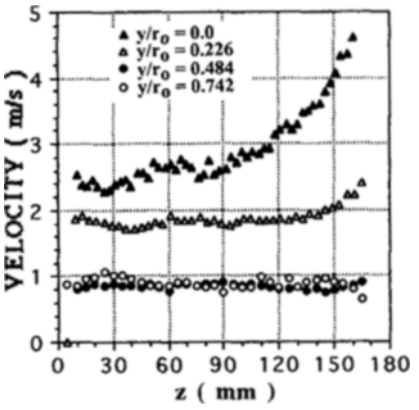

(a) Axial velocity

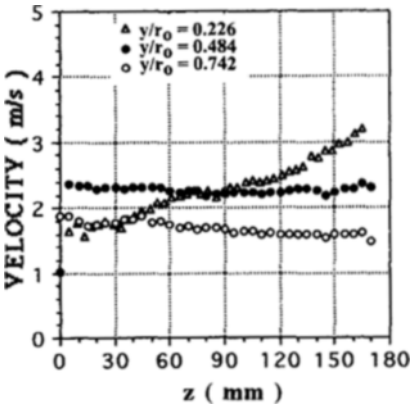

(b) Swirl velocity

Fig. 7 Variations of velocity along the streamwise direction (S.G.=60°)

$$=\frac{1}{t}[m' + V_d(\rho_{atm,2} - \rho_{atm,1}) + V_L(\rho_2 - \rho_1)] \quad (3)$$

and the discharge coefficients are calculated by

$$C_d = \frac{\dot{m}}{AC_* P_0 / (RT_0)^{0.5}} \quad (4)$$

The relative uncertainty associated with the calculation of the discharge coefficient of a sonic nozzle is determined as follows:

$$\frac{\delta C_d}{C_d} = \left[\left(\frac{\delta \dot{m}}{\dot{m}}\right)^2 + \left(\frac{\delta A}{A}\right)^2 + \left(\frac{\delta C_*}{C_*}\right)^2 + \left(\frac{\delta P_0}{P_0}\right)^2 + \frac{1}{2}\left(\frac{\delta T_0}{T_0}\right)^2 + \frac{1}{2}\left(\frac{\delta M}{M}\right)^2\right]^{0.5} \quad (5)$$

The mass flow rate, as defined in Eq (3), is determined by weighing the air that has been collected over a well-defined period of time. $\frac{\delta \dot{m}}{\dot{m}}$ is found to be less than ± 0.122 %. Among the studied sonic nozzles, the smallest nozzle has a throat diameter of 4.220 mm. When the diameter measurement error is ± 1 μm, $\frac{\delta A}{A}$ becomes ± 0.047 %. C_* is determined from the table and its error is ± 0.05 %. When the pressure is measured using a quartz bourdon gage, the measurement error is ± 0.025 %. However, the maximum error in pressure measurement is estimated as ± 0.125 % with the consideration of ± 1 kPa fluctuation at the test pressure of 1 MPa. Also, the maximum error in temperature measurement is estimated ± 0.041 %, including ± 0.1 ℃ fluctuations and ± 0.02 ℃ accuracy of PRT at 20 ℃ test temperature. The molecular weight of the air depends upon the composition change of the air, but its change is negligible. Consequently, overall uncertainty of the discharge coefficients measurement of a sonic nozzle is estimated as less than ± 0.2 %.

The discharge coefficients measured in this study for the toroidal throat nozzles, shown in Fig. 8, are presented in Fig. 9, where Reynolds number is defined by nozzle throat diameter and velocity at nozzle throat. Experimental data are compared with the values of ISO document (ISO, 1981). The discharge coefficients suggested in ISO document for the toroidal throat nozzle is given by the following equation.

$$C_d = 0.9935 - 1.525\ Re^{-0.5} \quad (10^5 < \mathrm{Re} < 10^7) \quad (6)$$

The dotted lines represent the $\pm$ 0.2 % bound of ISO values. Most of the experimental data fall within $\pm$ 0.2 % range which is expected from the uncertainty analysis. Therefore, the accuracy of the present gas flow measurement system is considered to be quite good.

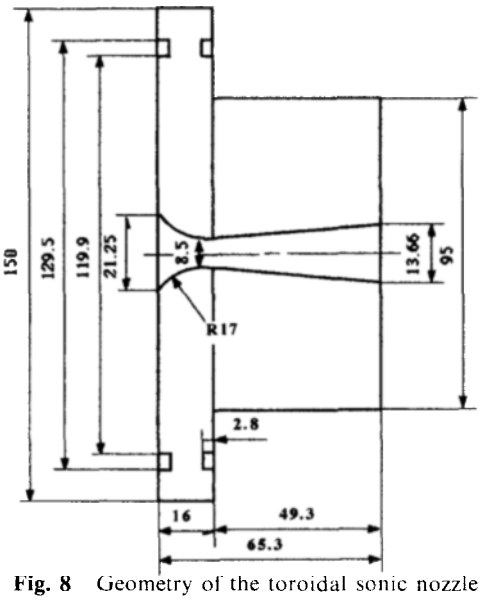

Fig. 8 Geometry of the toroidal sonic nozzle

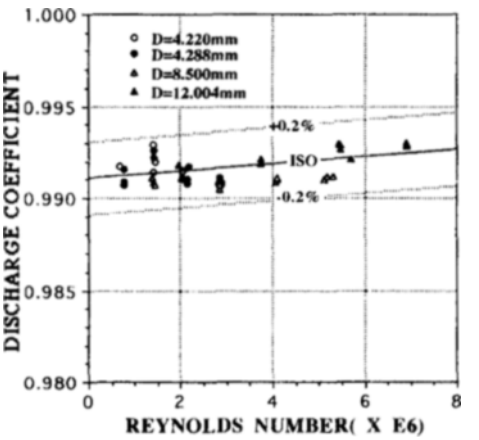

Fig. 9 Comparison of measured discharge coefficients with ISO values

3.3 Influence of swirl on discharge coefficient

The swirl generator is used to investigate the effects of upstream swirl on the discharge coefficients. Figure 10 shows the variation of the discharge coefficients measured with swirl generator for various nozzle throat diameters in terms of the

Table 1 Average errors of measured discharge coefficients comparing with ISO values

Swirl generator angle / Diameter(mm)	10°	20°	30°	40°	50°	60°	70°	80°
	%	%	%	%	%	%	%	%
4.285	+0.170	+0.118	+0.140	+0.167	+0.188	+0.192	+0.190	+0.217
8.501	+0.044	+0.057	+0.064	+0.124	+0.197	+0.367	+0.696	+1.385
12.004	−0.016	+0.001	+0.006	+0.120	+0.312	+0.648	+1.370	+2.981
16.980	−0.059	−0.028	+0.100	+0.189	+0.449	+1.162	+2.600	+4.936

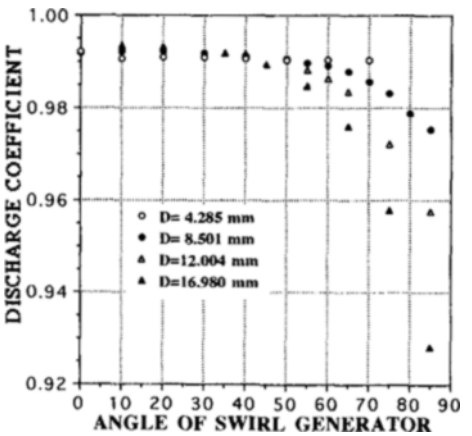

Fig. 10 Effect of upstream swirl on discharge coefficient

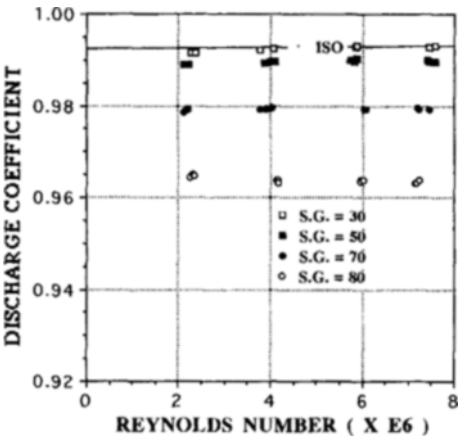

Fig. 11 Dependence of discharge coefficient on Reynolds number for various angles of swirl generator (D=12.004mm)

swirl generator angle. The upstream swirl does not have influence on the discharge coefficients of 4.285 mm nozzle, and the smallest throat diameter in the present study. For the angles of swirl generator less than 40°, variation of discharge coefficients is relatively small regardless of the nozzle throat diameter and the swirl generator angle. However, as the angle of swirl generator increases and the diameter of nozzle throat becomes larger, the discharge coefficients decrease gradually. Average errors of measured discharge coefficients comparing with ISO values are shown in Table 1 for various swirl angles and nozzle throat diameters.

Dependence of the discharge coefficients on Reynolds number for the various angles of swirl generator are presented in Fig. 11, and those are compared with ISO values. The experiments are performed with 12.004 mm nozzle for various inlet pressures. For all angles of swirl generator, slopes of the discharge coefficients are in good agreement with that of ISO document and the reproducibility of the data is seen to be very good. As the angle of swirl generator increases, however, the discrepancy between the experimental and ISO values becomes larger; +0.011~-0.113 % for the angle of 30°, 0.282~0.364 % for the angle of 50°, 1.358~1.410 % for the angle of 70° and 2.850~3.073 % for the angle of 80°.

The flow straightener, which is composed of six plate vanes, is installed upstream of sonic nozzle to reduce initial swirl. Figure 12 shows influence of upstream swirl on discharge coefficients under different swirl conditions. The discharge coefficients for the flow without straightener are somewhat higher than ISO values and the repeatability of the experimental data is worse than those obtained with straightener. The discharge coefficients measured with swirl generator for the angle of 50o are lower than ISO values, but the repeatability of the experimental data is better than those obtained with and without straightener.

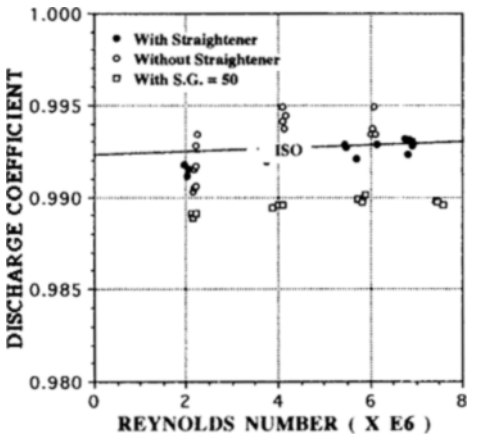

Fig. 12 Influence of upstream swirl on discharge coefficient under different swirl conditions (D=12.004 mm)

4. Conclusions

(1) As the angle of swirl generator becomes larger, axial velocity decreases around $r/r_0 \approx 0.5$ and increases in the pipe core, and swirl velocity increases. And both velocities at the core region increase when the flow approaches to the sonic nozzle.

(2) For the angle of swirl generator smaller than 40°, apparent swirling flow appears, and this influences the discharge coefficients.

(3) Overall uncertainty of the discharge coefficients measurement is estimated to be less than $\pm$ 0.2 %, and most of the experimental data fall within this range.

(4) For the angle of swirl generator less than 40°, variation of discharge coefficients is relatively small regardless of the nozzle throat diameter and the swirl generator angle.

(5) For all angles of the swirl generator, dependence of the discharge coefficients on Reynolds number is in good agreement with ISO value and repeatability of the data with swirl generator is seen to be better than those obtained with and without straightener.

References

Arnberg, B. T., 1962, "Review of Critical Flowmeters for Gas Flow Measurements," *J. of Basic Engineering*, Vol. 84. pp. 447~460.

Blake, K. A., Kinghorn, F. C. and Stevenson, R., 1981, "The Design of Flow Straightener/ Nozzle Package for Acceptance Testing of Air Compressors and Exhausters," *NEL Report*, No. 673.

Brown, E. F., Hamilton, G. L. and Kwok, D. W., 1985, "A Comparison of Three Critical Flow Venturi Designs," *J. of Fluids Engineering*, Vol. 107, pp. 316~321.

ISO, 1981, "Measurement of Gas Flow by Means of Critical Flow Venturi Nozzles," *Draft Proposal for ISO Standard Document*, ISO/ TC30/SC2/WG5.

Johnson, R. C., 1964, "Calculations of Real -Gas Effects in Flow through Critical-Flow nozzles," *J. of Basic Engineering*. Vol. 86, pp. 519~526.

Kinghorn, F. C., Mchugh, A. and Dyet, W. D., 1991, "The Use of toile Flow Straighteners with Orifice Plates in Swirling Flow," *Flow Measurement Instrument*, Vol. 2, pp. 162~168.

Smith, R. E. and Matz, R. J., 1962, "A Theoretical Method of Determining Discharge Coefficients for Venturis Operating at Critical Flow Conditions," *J. of Basic Engineering*, Vol. 84, pp. 434~446.